63. Electronic States of Phenylene and Naphthylene Bicyclobutanes. Linear Dichroism in Stretched Polyethylene

by **Jens Spanget-Larsen, Klaus Gubernator** and **Rolf Gleiter**

Institut für Organische Chemie der Universität, D-6900 Heidelberg 1

Erik W. Thulstrup

Department of Chemistry, Royal Danish School of Educational Studies, DK-2400 Copenhagen NV

and **Bernard Bianco, Gérard Gandillon** and **Ulrich Burger**

Départment de chimie organique de l'Université, CH-1211 Genève 4

(23.XII.82)

Summary

Excited singlet states of bicyclobutylene-benzene (**2**), 1,2:4,5-bis(bicyclobutylene)benzene (**3**), 2,3-bicyclobutylene-naphthalene (**4**), and 1,8-bicyclobutylene-naphthalene (**5**) are investigated by means of linear dichroic absorption spectroscopy of molecules oriented in stretched polyethylene films and by semi-empirical model calculations. The results indicate a strong hyperconjugative impact of the bicyclobutylene group on the aromatic chromophores in these compounds. Valence isomerization to aromatic products is predicted as the preferred photochemical pathway.

Introduction. – Since the publication of the convenient synthesis of benzvalene (**1**) and its homologues by *Katz, Wang & Acton* [1] in 1971, the chemistry and spectroscopy of this interesting class of bicyclo[1.1.0]butane derivatives have been intensively investigated [2] [3]. In a recent photoelectron (PE.) spectroscopic investigation it was found that bicyclobutylene substitution may have a very strong impact on the π-electronic structure of an aromatic hydrocarbon [4]. In the

1 2 3

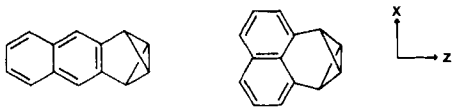

4 5

present work we study the influence of bicyclobutylene substitution on the electronically excited states of benzene and naphthalene, by means of linear dichroic (LD.) absorption spectroscopy and model calculations on the phenylene and naphthylene bicyclobutanes **2**–**5**. As we shall demonstrate, hyperconjugative interactions with bicyclobutane *Walsh*-orbitals can explain the observed differences in the UV. spectra of these compounds

Observed LD. spectra. – Samples of **2**–**5** were synthesized according to directions in the literature [1] [4–6] and their LD. absorption spectra in stretched polyethylene were measured on a *Cary 17D* spectrometer according to the TEM procedure [7–9]. UV. absorption data measured in liquid solution have been published previously for **2** [1] and **5** [6].

In the case of **2** and **3** the observed spectra indicated the presence of impurities. The spectrum of **2** thus contained a peak close to 45 000 cm^{-1} corresponding to the intense naphthalene ^1B_b-band ($\log\varepsilon = 5.1$); the estimated amount of naphthalene impurity is around 0.5%. The naphthalene contributions were removed from the observed LD. absorption curves $E_\parallel^I(\tilde{\nu})$ and $E_\perp^I(\tilde{\nu})$ by subtraction of appropriately scaled naphthalene LD. absorption curves $E_\parallel^N(\tilde{\nu})$ and $E_\perp^N(\tilde{\nu})$, thereby obtaining the curves $E_\parallel^P(\tilde{\nu})$ and $E_\perp^P(\tilde{\nu})$ corresponding to pure **2**:

$$E_\parallel^P(\tilde{\nu}) = E_\parallel^I(\tilde{\nu}) - c\,E_\parallel^N(\tilde{\nu})$$

$$E_\perp^P(\tilde{\nu}) = E_\perp^I(\tilde{\nu}) - c\,E_\perp^N(\tilde{\nu})$$

The absorption curves for naphthalene were recorded independently, using a similar sheet of stretched polyethylene at 77 K, and the scaling factor c was chosen such that the naphthalene peak at 45 000 cm^{-1} just vanished from the resulting curves $E_\parallel^P(\tilde{\nu})$ and $E_\perp^P(\tilde{\nu})$; for this purpose a computerized 'stepwise reduction procedure' was applied.

In the case of **3**, only a characteristic benzenoid absorption band with onset at 33 700 cm^{-1} and a shape very similar to that of the corresponding band of **2** could be safely assigned to an absorption of **3**. Towards higher energies relatively strong absorption with prominent maxima at 38 600 and 43 700 cm^{-1} was observed. However, leaving a sample of **3** dissolved in polyethylene for four days at room temperature lead to disappearance of the benzenoid band at 33 700 cm^{-1}, while the peaks at 38 600 and 43 700 remained. This indicates to us that the latter absorption is mainly due to impurities, probably including thermolytic rearrangement products of **3** (the compound rearranges with $t_{1/2}$ (70°) = 15 min to 1,5- and 1,7-dimethylidene-1,5- resp. 1,7-dihydro-*s*-indacene [5]). No attempt was made to correct numerically for the absorption of impurities in this case.

The reduced absorption curves [9]

$$A_1(\tilde{\nu}) = [(1-K_2)\,E_\parallel(\tilde{\nu}) - 2\,K_2\,E_\perp(\tilde{\nu})]/(K_1-K_2)$$

$$A_2(\tilde{\nu}) = [2\,K_1\,E_\perp(\tilde{\nu}) - (1-K_1)\,E_\parallel(\tilde{\nu})]/(K_1-K_2)$$

for **2** and **4** are shown in *Figure 1* and *2*. In the case of **2** the reduction factor d_1 (which removes long-axis polarized intensity from the linear combination

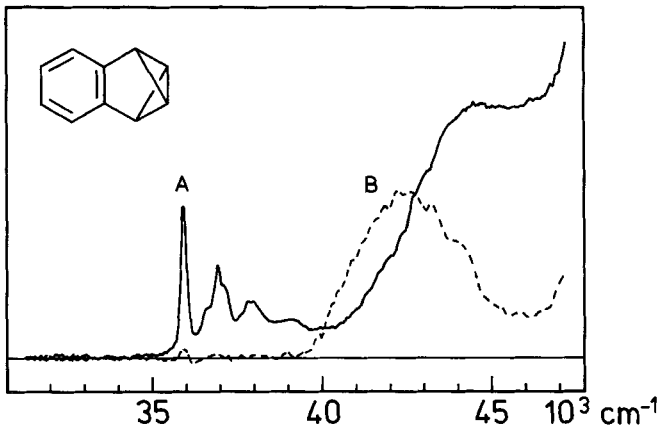

Fig. 1. *Polarized absorption spectrum of bicyclobutylene-benzene (2) at 77K in stretched polyethylene.* The *Figure* shows the reduced absorption curves $A_z = E_\parallel - 1.0\ E_\perp$ (full line) and $A_x = 1.50\ E_\perp - 0.75\ E_\parallel$ (broken line), where $E_\parallel$ and $E_\perp$ are the absorption curves measured with the stretching direction *parallel* and *perpendicular* to the plane of the linearly polarized light.

$E_\parallel - d_1 E_\perp$) and thereby the orientation factor $K_1 = d_1/(d_1+2)$ [9] was determined under the assumption that the peak A at 36000 cm^{-1} is long-axis polarized, leading to $d_1 = 2.0$ and $K_1 = 0.50$. The reduction factor d_2 and the orientation factor $K_2 = d_2/(d_2+2)$ [9] cannot be estimated directly from the LD. spectrum because of the absence of a suitable short-axis polarized peak. The curves in *Figure 1* were produced with the reduction factors $(d_1, d_2) = (2.0, 1.0)$, corresponding to a point $(K_1, K_2) \approx (0.50, 0.33)$ close to the 'centre' of the orientation triangle [8] [9]; the

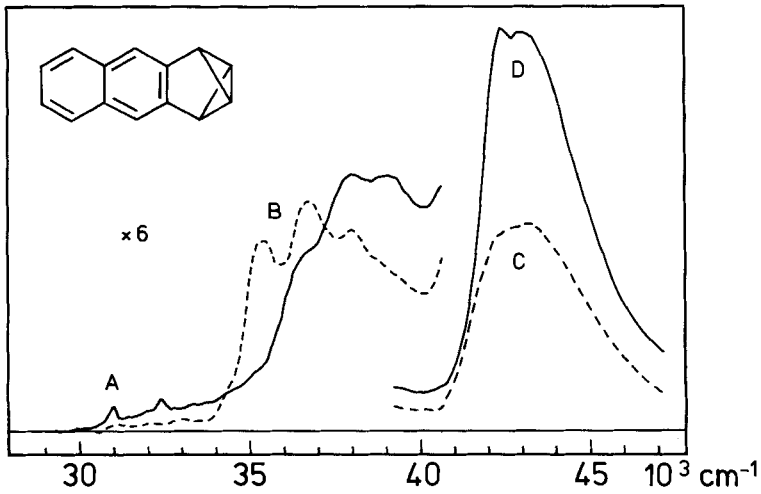

Fig. 2. *Polarized absorption spectrum of 2,3-bicyclobutylene-naphthalene (4) at room temperature in stretched polyethylene.* The *Figure* shows the reduced absorption curves $A_z = E_\parallel - 0.70\ E_\perp$ (full line) and $A_x = 1.93\ E_\perp - 0.38\ E_\parallel$ (brocken line). See legend to *Figure 1*.

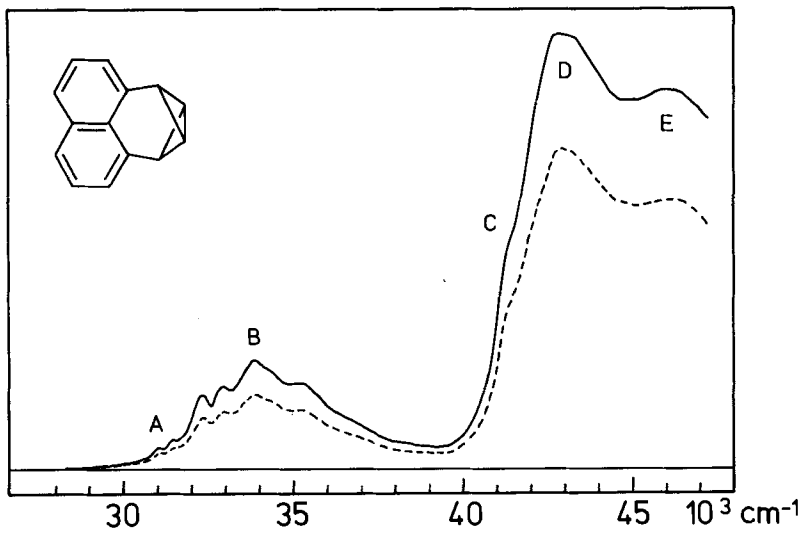

Fig. 3. *Polarized absorption spectrum of 1,8-bicyclobutylene-naphthalene (5) at room temperature in stretched polyethylene.* The *Figure* shows the observed, *unreduced* absorption curves $E_{\parallel}$ and $E_{\perp}$. See legend to *Figure 1.*

essential conclusions do not depend critically on the assumptions made. In the case of **4** the reduction factors were determined under the assumptions that the peak A at 31000 cm^{-1} is long-axis polarized and the peak B at 35300 cm^{-1} is short-axis polarized, leading to $(d_1, d_2) = (5.0, 0.70)$ and $(K_1, K_2) \approx (0.71, 0.26)$. These values indicate that the orientation distribution is far from 'rod-like' since $K_1 \neq 1 - 2K_2$ [7–9]. In contrast, the valence isomer anthracene behaves essentially like a cylindrical rod in a similar sheet, $(K_1, K_2) \approx (0.62, 0.20)$ [10], suggesting that in the case of **4** the bicyclobutane fragment has a significant influence on the orientation mechanism.

The observed absorption curves $E_{\parallel}(\tilde{\nu})$ and $E_{\perp}(\tilde{\nu})$ for **5** are shown in *Figure 3.* In this case the LD. is less interesting since $E_{\parallel}(\tilde{\nu}) \approx 1.4\ E_{\perp}(\tilde{\nu})$, indicating that the orientation is of the 'disk-like' limiting type [7–9] with $K_1 = K_2 \approx 0.42$. This result is not surprising in view of the shape of this molecule and is consistent with observed orientation factors for planar naphthylene derivatives [8].

Discussion and comparison with theory. – Observed band maxima for **2**–**5** are indicated and compared with calculated transitions in the *Table.* In the following we consider the assignment of the observed transitions and the shifts observed relative to the corresponding transitions in benzene and naphthalene; for discussions of the UV. spectra of benzenoid hydrocarbons we refer to [11–16] and literature cited there.

The benzene derivatives **2** *and* **3.** It is generally agreed that the two lowest energy transitions in benzene are to $^1B_{2u}$- and $^1B_{1u}$-states, corresponding to ^1L_b- and ^1L_a-states according to *Platt* [11]. In D_{6h}-benzene both transitions are electronically

Table. *Observed and calculated transitions for* **2**–**5**. The *Table* indicates observed wavenumbers $\tilde{\nu}_{max}$ in units of 1000 cm^{-1}, (logε)-values (cyclohexane) and polarization directions p. Calculated results are given with inclusion of singly excited configurations (SCI.) and with inclusion of singly and doubly excited configurations (SDCI.).

Cpd.		Obs.			Calc. (SCI.)			Calc. (SDCI.)		
		$\tilde{\nu}$	logε	p	Sym-metry	$\tilde{\nu}$	logε [a]	$\tilde{\nu}$	logε [a]	Leading configurations
2	A[b]	36.0	2.7	z	$^1A_1$ (L_b)	35.5	2.8	34.1	2.7	$4b_2 \rightarrow 5b_2$ (59%), $2a_2 \rightarrow 3a_2$ (34%)
	B[c]	42.5	(3.0)	x	$^1B_1$ (L_a)	37.8	3.5	39.2	3.6	$4b_2 \rightarrow 3a_2$ (88%), $2a_2 \rightarrow 5b_2$ (9%)
3	A[b]	33.7	–	z	$^1B_{1u}$ (L_b)	32.3	3.2	30.7	3.0	$3b_{3g} \rightarrow 4b_{2u}$ (64%), $2b_{1g} \rightarrow 2a_u$ (28%)
	B	–	–	–	$^1B_{3u}$ (L_a)	35.6	3.8	37.6	3.8	$3b_{3g} \rightarrow 2a_u$ (94%)
4	A[b]	31.0	2.5	z	$^1A_1$ (L_b)	31.2	1.9	32.4	2.4	$5b_2 \rightarrow 6b_2$ (53%), $3a_2 \rightarrow 4a_2$ (42%)
	B	36.6	3.3	x	$^1B_1$ (L_a)	34.1	2.7	35.6	2.9	$3a_2 \rightarrow 6b_2$ (63%), $5b_2 \rightarrow 4a_2$ (34%)
	C	43	4.0	x	$^1B_1$ (B_a)	41.5	4.3	42.6	4.2	$5b_2 \rightarrow 4a_2$ (57%), $3a_2 \rightarrow 6b_2$ (30%)
	–	–	–	–	$^1A_1$	42.3	4.2	43.2	2.3	$5b_2 \rightarrow 7b_2$ (67%), $2a_2 \rightarrow 4a_2$ (20%)
	D	43	4.3	z	$^1A_1$ (B_b)	42.9	4.7	44.2	4.8	$3a_2 \rightarrow 4a_2$ (52%), $5b_2 \rightarrow 6b_2$ (43%)
5	A[b]	31.0	3.1[d]	–	$^1B_1$ (L_b)	31.6	2.9	33.9	2.8	$3a_2 \rightarrow 6b_2$ (61%), $5b_2 \rightarrow 4a_2$ (34%)
	B	33.9	3.9	–	$^1A_1$ (L_a)	33.4	3.8	35.6	3.8	$3a_2 \rightarrow 4a_2$ (86%), $5b_2 \rightarrow 6b_2$ (10%)
	C	(41)	–	–	$^1B_1$	39.7	3.6	41.9	3.1	$3a_2 \rightarrow 7b_2$ (81%), $5b_2 \rightarrow 4a_2$ (7%)
	D	42.7	4.5	–	$^1B_1$	43.4	4.4	43.7	4.0	$4b_2 \rightarrow 4a_2$ (51%), $5b_2 \rightarrow 4a_2$ (26%)
	–	–	–	–	$^1A_1$	43.0	2.2	44.8	2.1	$4b_2 \rightarrow 6b_2$ (42%), $5b_2 \rightarrow 7b_2$ (41%)
	–	–	–	–	$^1A_2$	43.4	–	46.9	–	$14a_1 \rightarrow 4a_2$ (93%)
	E	46.1	4.5	–	$^1B_1$	45.4	4.2	47.3	4.5	$4b_2 \rightarrow 4a_2$ (38%), $5b_2 \rightarrow 4a_2$ (27%)
	–	–	–	–	$^1A_1$	45.9	4.2	48.3	4.0	$5b_2 \rightarrow 6b_2$ (76%), $4b_2 \rightarrow 7b_2$ (11%)

[a] Estimated by the relation logε = 4.74 + log$f$ [25].
[b] Observed band origin.
[c] These data correspond to a shoulder in the liquid solution spectrum [1].
[d] Logε values for **5** are taken from [6].

forbidden by symmetry, but they appear in the spectrum due to intensity borrowed from the intense $^1E_{1u}$-transition in the vacuum UV. by vibronic interactions. In the case of an *ortho*-disubstituted benzene derivative (point group C_{2v}), the ^1L-transitions become electronically allowed and the transitions corresponding to the benzene ^1L_b- and ^1L_a-bands are polarized parallel and perpendicular, respectively, to the symmetry axis of the molecule. For **2** we thus expect two bands in the near UV. region, corresponding to a long-axis polarized ^1L_b- and a short-axis polarized ^1L_a-transition, and similar bands are expected for **3**.

Assignment of band A of **2** to the ^1L_b-transition is straight-forward. The band has a prominent zero-zero peak at 36000 cm^{-1} and a shape very similar to that of the corresponding bands of related species such as indane and tetralin [15]. The diffuse absorption B with onset close to 40000 cm^{-1} can be assigned to the ^1L_a-transition. While the ^1L_b-band is almost purely long-axis polarized, the ^1L_a-band shows strongly mixed polarization with a broad short-axis polarized maximum at 42500 cm^{-1} overlapping the onset of more intense long-axis polarized absorption. This situation is not unlike that encountered for other benzene derivatives (see, *e.g.*, [16]). The long-axis polarized component of the ^1L_a-band of **2** is most likely of vibronic origin, involving non-totally symmetric vibrations.

The assignment of the ^1L-bands of **2** is consistent with the calculated CNDO-CI results. The predicted transition energies are slightly too low, but, more significantly,

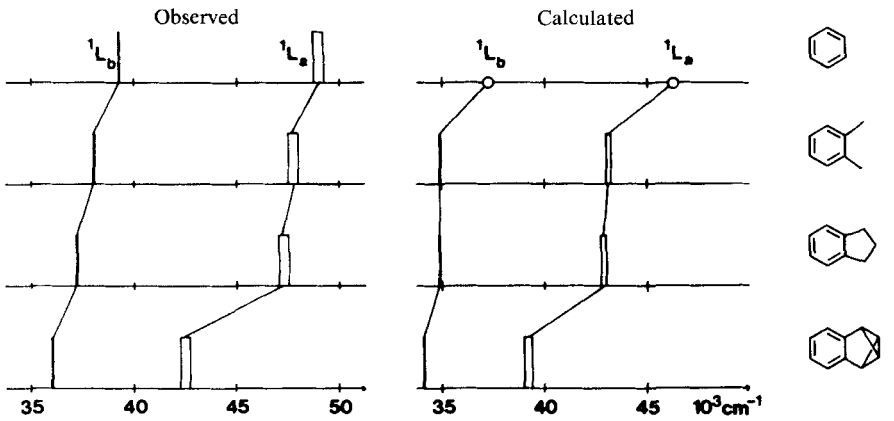

Fig. 4. *Comparison of observed* (left) *and calculated* (right) *transition energies for benzene, o-xylene, indane* [15] *and bicyclobutylene-benzene (2).* The thickness of the bars indicates relative intensity, circles indicate electronic transitions forbidden by symmetry.

the trends in a series of related compounds comprising benzene, *o*-xylene, indane and **2** are well predicted as shown in *Figure 4.* The most remarkable feature is the large red shift of the ^1L_a-band in the case of **2**. According to the calculation, this can be explained as a result of the strong hyperconjugative destabilization of the $4b_2$-HOMO and a slight destabilization of the $3a_2$-LUMO. These effects, which have been previously discussed in detail [4], lead to a considerable decrease of the energy of the HOMO → LUMO configuration which becomes the dominant contribution to the ^1L_a-state of **2** in the CI. description *(Table 1).* A strong red shift of the ^1L_a-band is generally characteristic for benzene derivatives with conjugating substituents, *e.g.*, styrene, indene, *etc.* [15], where the so-called conjugation band is considered to be due to the HOMO → LUMO transition [11–14].

The hyperconjugative effects operating in **2** are magnified in **3**, leading to further energy lowering of the predicted ^1L-transitions *(Table 1).* The prediction can be verified experimentally in case of the ^1L_b-transition which is clearly observed with an onset at 33700 cm^{-1}; the position of the ^1L_a-band is obscured by the presence of impurities, as discussed in the previous section.

The naphthalene derivatives **4** *and* **5**. Both spectra start with a weak absorption band A with onset at 31000 cm^{-1}, overlapping a medium intense complex band B with maximum at 34–37000 cm^{-1}. We assign these bands to transitions corresponding to the ^1L_b- and ^1L_a-transitions of naphthalene, in agreement with the calculated results and the polarization directions observed for **4**. The ^1L_a-band of the latter compound shows mixed polarization in the 35–40000 cm^{-1} region, strongly reminiscent of the ^1L_a-band of **2**. In the case of **4**, two overlapping mutually perpendicularly polarized vibronic progressions are observed. The origin close to 35000 cm^{-1} is short-axis (x) polarized, consistent with the electronic symmetry of the transition, while the long-axis polarized progression can be assigned to vibronic components involving non-totally symmetric vibrations and probably gaining intensity by vibronic coupling with the intense transitions at higher energies. Unfortunately, the LD. observed for **5** prevents a detailed discussion in this case.

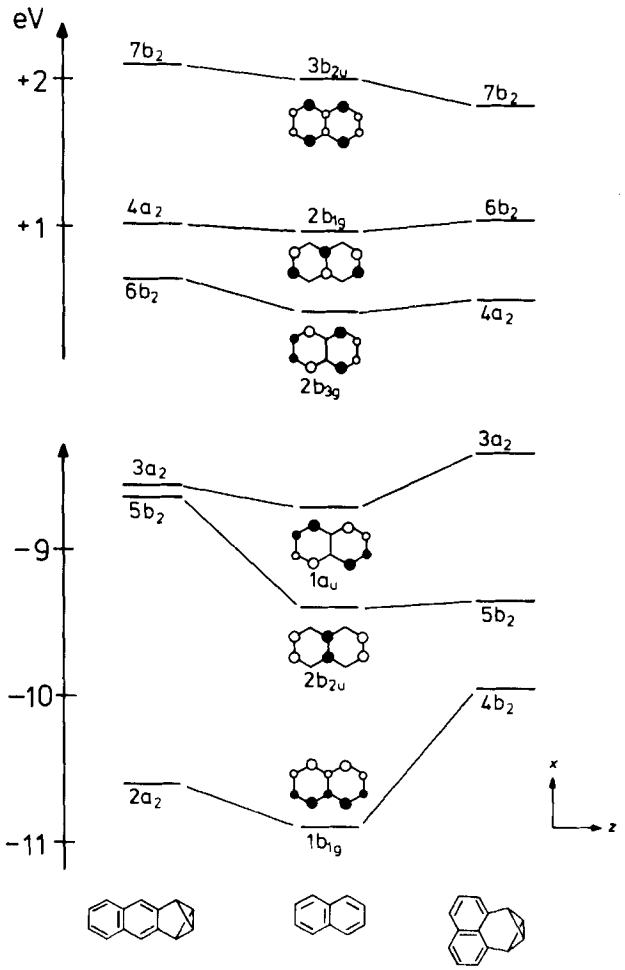

Fig. 5. *Correlation of the three highest occupied and three lowest unoccupied orbital energies for naphthalene, 2,3-bicyclobutylene- and 1,8-bicyclobutylene-naphthalene* (**4** resp. **5**) *calculated by the CNDO method*

In the region above 40 000 cm^{-1} observed as well as calculated spectra of **4** and **5** show significant differences, indicating a strong dependence on the mode of linkage. In the case of **4**, the overlapping intense bands C and D with maxima close to 43 000 cm^{-1} can easily be assigned to ^1B_a- and ^1B_b-transitions, respectively, but in the case of **5** the situation is much more complicated. In order to trace the origin of these differences, we have worked out the calculated correlation diagrams in *Figures 5* and *6*.

The shifts of the three highest occupied and the three lowest unoccupied orbitals of naphthalene when going to **4** or **5** are indicated in *Figure 5*. The large shifts of the occupied levels are verified experimentally by PE. spectroscopy and have been discussed previously [4]; the shifts of the unoccupied levels are much

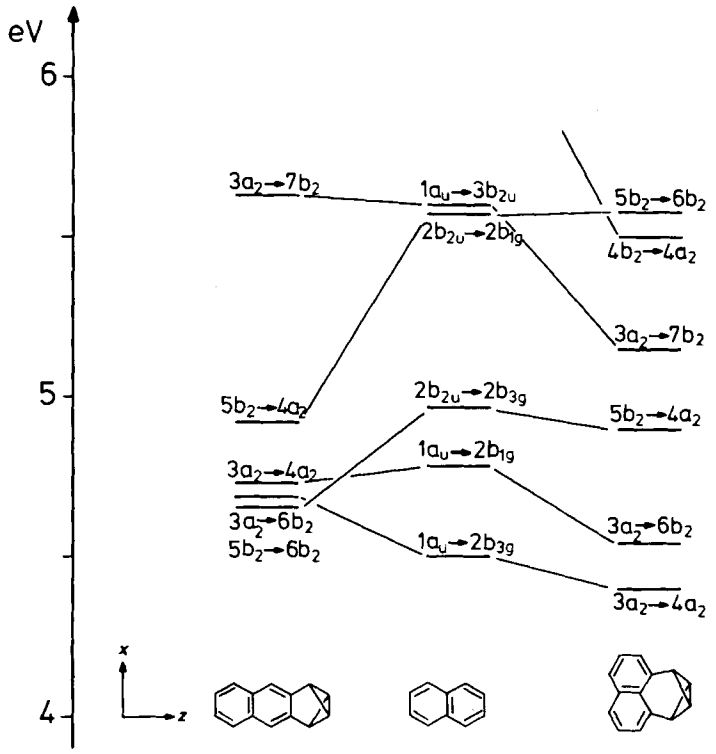

Fig. 6. *Correlation of low energy monoexcited singlet configuration energies for naphthalene, 2,3-bicyclobutylene- and 1,8-bicyclobutylene-naphthalene* (**4** resp. **5**) *calculated by the CNDO method*

smaller. Now, in the case of **4** it is evident that the two highest occupied as well as the two lowest unoccupied levels become near-degenerate and well separated from other orbital energy levels, resulting in a pattern similar to that found in a slightly perturbed [4n+2]annulene. In the case of **5**, however, the trend is quite different; the third highest occupied and the third lowest unoccupied level are shifted in direction of the frontier levels, thereby complicating the energy level-pattern in the frontier region.

The energies of the lowest excited singlet configurations are correlated in the diagram in *Figure 6*. The trends of the diagram are consistent with what would be expected on the basis of the results shown in *Figure 5*. In the case of **4** a group of four closelying configurations at low energy is separated considerably in energy from configurations at higher energies. As a consequence, the low energy region of the calculated spectrum is dominated by the four states derived by interaction of the four low energy configurations, and these states closely correspond to ^{1}L- and ^{1}B-states in *Platt*'s perimeter model [11]. Hence, in a sense, the perturbation due to the interaction with bicyclobutane *Walsh*-orbitals tends to oppose the influence of the *transannular* naphthalene bond, rendering the spectral properties of **4** similar to those of a naphthalene shaped [10]annulene [17]. As indicated in *Figure 7*, the most significant shift relative to naphthalene is the predicted reversal of the ordering

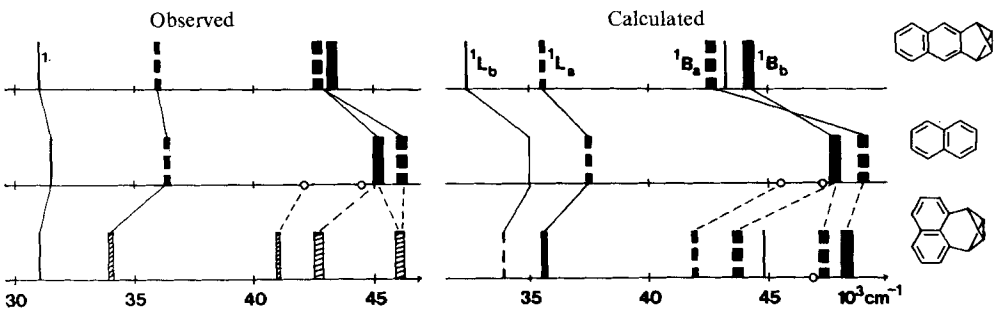

Fig. 7. *Comparison of observed* (left) *and calculated* (right) *transition energies for naphthalene, 2,3-bicyclobutylene- and 1,8-bicyclobutylene-naphthalene* (**4** resp. **5**). Full bars indicate z-polarized, broken bars x-polarized transitions. The thickness indicates relative intensity; transitions forbidden by symmetry are indicated by circles. Observed data for naphthalene are taken from [15] [18–20]. In the case of **5**, observed polarization directions are not available.

of the ^1B_b- and ^1B_a-states, resulting in ^1B_a below ^1B_b. This is consistent with the spectral evidence for **4** since the onset of the short-axis polarized ^1B_a-band (C) seems to be slightly below that of the long-axis polarized ^1B_b-band (D) *(Fig. 2)*. It is interesting to note that the ordering of the ^1B-states (^1B_a below ^1B_b) has been verified by MCD. spectroscopy in the case of 1,6-methano[10]annulene [21], thereby emphasizing the parallelism between **4** and a deformed [10]annulene.

In the case of **5** there is no obvious similarity to the situation in [10]annulene. In fact, only the two lowest calculated transitions can meaningfully be assigned to transitions in the perimeter model, namely the ^1L_b- and ^1L_a-transitions. The states at higher energy generally seem to contain several important contributions. They cannot easily be classified as B-states and the correlation with the excited states of naphthalene is not obvious. This is due to the presence of additional low energy configurations, such as $3a_2 \rightarrow 7b_2$ and $4b_2 \rightarrow 4a_2$ *(Fig. 6)* which interact strongly with $5b_2 \rightarrow 4a_2$ and introduce additional transitions between 40000 and 50000 cm^{-1}. The third excited state of **5** predicted close to 42000 cm^{-1} is fairly well described by the $3a_2 \rightarrow 7b_2$ configuration. The shoulder at 41000 cm^{-1} (C) can probably be assigned to this state. It may correspond to the third excited singlet state of naphthalene which is optically forbidden in ordinary one-photon absorption spectroscopy but is clearly observed in the two-photon spectrum (42100 cm^{-1}) [20]. In the case of acenaphthene the transition gives rise to a well resolved peak in the standard solution spectrum (41000 cm^{-1}, $\log\varepsilon = 3.1$) [15] [20]. The strong bands in the spectrum of **5** with maxima close to 43000 and 46000 cm^{-1} seem well predicted by the calculation as the result of several strong transitions. More definite conclusions would require additional experimental information and we shall refrain from further analysis at this time.

Concluding remarks. – Benzvalene and its homologues are known to undergo a number of isomerization reactions [2] [3] [5]. In connection with the present investigation it is of interest to estimate the probable photochemical rearrangement products. Inspection of the calculated wavefunctions indicates that excitation into a low-lying excited state is associated with transfer of electron density from the b_2

and a_2 bicyclobutane *Walsh*-orbitals into the π-system. The b_2 and a_2 *Walsh*-orbitals are anti-bonding with respect to the central 1,3-bicyclobutane bond, but bonding in the remaining positions [4] [22]. This means that the 1,3-bond should be strengthened and the remaining C,C-bonds weakened on excitation. This, in turn, speaks against a photochemical rearrangement involving breaking of the 1,3-bicyclobutane bond, *e.g.*, isomerization to fulvene derivatives in the case of **1–4**. Valence isomerization to aromatic products (pleiadiene in the case of **5**) is predicted as the preferred photochemical pathway, in contrast to most thermally induced rearrangements [2] [3] [5]. This prediction should be most reliable in those cases where the hyperconjugative effects are particularly strong, *e.g.*, in the case of **1–3**. The observed photochemical rearrangement of **1** to benzene [23] is consistent with our prediction. It is also interesting that methoxy-azulvalene has been found to undergo clean isomerization to methoxy-azulene on irradiation [24], in accordance with our expectation.

Calculations. – CNDO-CI. calculations on **2–5** and a number of related compounds were carried out using the program written by *Baumann* [25]. All geometries were taken as those predicted by MINDO/3 [26] [27]; C_{2v}-symmetry was assumed for the bicyclobutane compounds (D_{2h} for **3**). The standard parameters stored in the computer program were employed [25] and selection of configurations for the CI. expansion was carried out as described previously [28].

We thank the *Deutsche Forschungsgemeinschaft*, the *Schweizerische Nationalfonds zur Förderung der wissenschaftlichen Forschung*, the *Fonds der Chemischen Industrie* and the *BASF, Ludwigshafen*, for the financial support.

REFERENCES

[1] *T.J. Katz, E.J. Wang & N. Acton*, J. Am. Chem. Soc. *93*, 3782 (1971).
[2] *U. Burger*, Chimia *33*, 147 (1979).
[3] *M. Christl*, Angew. Chem. *93*, 515 (1981); Angew. Chem. Int. Ed. *20*, 529 (1981).
[4] *R. Gleiter, K. Gubernator, M. Eckert-Maksič, J. Spanget-Larsen, B. Bianco, G. Gandillon & U. Burger*, Helv. Chim. Acta *64*, 1312 (1981).
[5] *G. Gandillon, B. Bianco & U. Burger*, Tetrahedron Lett. *1981*, 51.
[6] *I. Murata & K. Nakasuji*, Tetrahedron Lett. *1973*, 47; *R.M. Pagni & C.R. Watson*, ibid. *1973*, 59.
[7] *E.W. Thulstrup, J. Michl & J.H. Eggers*, J. Phys. Chem. *74*, 3868 (1970); *J. Michl, E.W. Thulstrup & J.H. Eggers*, ibid. *74*, 3878 (1970).
[8] *E.W. Thulstrup & J. Michl*, J. Am. Chem. Soc. *98*, 4533 (1976).
[9] *E.W. Thulstrup & J. Michl*, J. Phys. Chem. *84*, 82 (1980); J. Am. Chem. Soc. *104*, 5594 (1982); *E.W. Thulstrup*, 'Aspects of the Linear and Magnetic Circular Dichroism of Planar Organic Molecules', Springer-Verlag, Berlin 1980.
[10] *J. Michl, E.W. Thulstrup & J.H. Eggers*, Ber. Bunsenges. Physik. Chem. *78*, 575 (1974).
[11] *J.R. Platt*, J. Chem. Phys. *17*, 484 (1949); *J.R. Platt, K. Ruedenberg, C.W. Scherr, J.S. Ham, H. Labhart & W. Lichten*, 'Free-Electron Theory of Conjugated Molecules: A Source Book', Wiley, London 1964.
[12] *J.N. Murrell*, 'The Theory of the Electronic Spectra of Organic Molecules', Methuen & Co., London 1963.
[13] *H. Suzuki*, 'Electronic Absorption Spectra and Geometry of Organic Molecules', Academic Press, New York 1967.

[14] Papers by *H.-H. Perkampus & F. Dörr*, in: Ref. [15].
[15] 'UV Atlas of Organic Compounds', Butterworths, London 1971.
[16] *E. W. Thulstrup, M. Vala & J. H. Eggers*, Chem. Phys. Lett. *7*, 31 (1970); *E. W. Thulstrup*, Int. J. Quant. Chem. IIIs, 641 (1970); J. Mol. Struct. *47*, 359 (1978).
[17] *H.-R. Blattmann, W. A. Böll, E. Heilbronner, G. Hohlneicher, E. Vogel & J.-P. Weber*, Helv. Chim. Acta *49*, 2017 (1966).
[18] *E. W. Thulstrup*, Thesis, Aarhus University 1966.
[19] *M. Vasák, M. R. Whipple & J. Michl*, J. Am. Chem. Soc. *100*, 6838 (1978).
[20] *B. Dick & G. Hohlneicher*, Chem. Phys. Lett. *84*, 471 (1981).
[21] *H. J. Dewey, H. Deger, W. Fröhlich, B. Dick, K. A. Klingensmith, G. Hohlneicher, E. Vogel & J. Michl*, J. Am. Chem. Soc. *102*, 6412 (1980).
[22] *P. Bischof, R. Gleiter & E. Müller*, Tetrahedron *32*, 2769 (1976).
[23] *C. A. Renner, T. J. Katz, J. Pouliquen, N. J. Turro & W. H. Waddell*, J. Am. Chem. Soc. *97*, 2568 (1975).
[24] *Y. Sugihara, T. Sugimura & I. Murata*, J. Am. Chem. Soc. *104*, 4295 (1982).
[25] *H. Baumann*, QCPE *10*, 333 (1977).
[26] *R. C. Bingham, M. J. S. Dewar, D. H. Lo*, J. Am. Chem. Soc. *97*, 1285 (1975).
[27] *P. Bischof*, J. Am. Chem. Soc. *98*, 6844 (1976); QCPE *12*, 383 (1979).
[28] *J. Spanget-Larsen & R. Gleiter*, Helv. Chim. Acta *61*, 2999 (1978).